Indonesian Journal of Electrical Engineering and Computer Science
Vol. 20, No. 3, December 2020, pp. 1693~1702
ISSN: 2502-4752, DOI: 10.11591/ijeecs.v20.i3.pp1693-1702

Harmonic spectra of BLDC motor supplied by a solar PV

Afaneen Anwer Abbood
Department of Electrical Engineering, University of Technology (UOT), Iraq

Article Info

Article history:

Received Apr 17, 2020
Revised May 19, 2020
Accepted Jun 5, 2020

Keywords:

BLDC motor
Harmonic distortion
Multilevel inverter
Space-vector modulation

ABSTRACT

The multilevel inverters have been used especially in renewable energy aspects in order to assess total harmonic distortion (THD). THD is considered to produce a good quality of current signal of BLDC motor drive. In this paper, a solar PV inveter fed brushless DC (BLDC) motor drive is discussed considering two topologies of three phase multilevel inverters. These topologies are flying capacitor and clamped diode inverters. The inverter efficiency and output power have an effectiveness on THD values. A boost dc to dc converter using incremental conductance maximum power point tracking (INC-MPPT) is implemented with a solar PV. The mathematical model of the proposed systems ares tudied via simulation using Matlab/Simulink. The simulation results of a BLDC motor based on two multilevel inverters are compared with each other considering the THD and the utilization of the dc-bus voltage, the comparition verified that the clamped diode inverter has a better harmonic spectra.still the overshoot is a little bit high in the two types of inverter that are proposed.

Corresponding Author:

Afaneen Anwer Abbood,
Department of Electrical Engineering,
University of Technology, Electrical Department, Iraq.
Email: 30237@uotechnology.edu.iq

1. INTRODUCTION

The motivation of increasing use of BLDC motor in many applications such as: computer hard disk drives, military and insdustrial. This is due to an improvement of permanent magnet construction as well as the improvement of the power electronic devices. Moreover, the motor design cost is rapidly decreasing. Therefore, it has been illustrated that in the past few years the BLDC motors are utilized in different applications starting from the simple ones like pumps or fans to high performance drives like machine-tools servos and applications that require high level of speed regulation like hybrid electric vehicles. This is all because this type of motors contains special features such as high torque to inertia ratio, high reliability, low cost, and high power per weight ratio [1].

Recently multilevel inverters have been used especially in renewable energy aspects in order to assess THD [2-5]. Two topologies of three-phase inverter are tested and implemented with BLDC motor drive. These topologies are the flying capacitor inverter and clamped diode inverter [6-7]. Amol K. Koshti, M. N. Rao (2017) [8] discussed the different multilevel inverter (MLI) topologies review including diode clamped multilevel DC-MLI) inverter, flying capacitor multilevel FC-MLI) inverter, cascaded H-bridge (CHB)converter and it introduced their applications in renewable energy [9-11].

A space vector pwm (SVPWM) controlled the inverter schemes [12-13]. In spite of the limitations of PWM techniques that the carrier phase shift (CPS-PWM) and carrier in-phase disposition (IPD-PWM) modulation techniques can be implemented to Cascaded H-bridge multilevel inverters [14-15]. In order to assess THD, repeated measures were used. Hence, the previous studies have been based their criteria for selection on type of multilevel inverter and on the other hand in most recent studies THD has been measured for different inverter type modification. Just over 5% of THD was acceptable [16-18].

The power quality of the voltage and current signals is improved according to the number of inverter level [19]. Since the output is closer to sinusoidal wave. Consequently, the inverter efficiency and output power have an effectiveness on THD values. Therefore, it is important to modify the inverter topology gaining acceptable output signals.

Moreover, an incremental conductance algorithm has been used to improve the system performance obtaining a maximum power point tracking (MPPT) from the PV panel. The DC supplies will provide from a PV solar array [20]. Reference [21] improved the output line voltage harmonic characteristics by combining a hybrid of these above-mentioned two techniques. In addition, due to the higher dv/dt output from the switching devices in inverters those results from a high dc link voltage, a multi domain dv/dt filters is designed [18]. Modulation index and power factor are maintained in order to increase the balance of the NP voltage by presenting an efficiency-optimized dual modulation wave carrier-based PWM (DMWPWM) strategy of three-level NPC inverter [22]. Some researches implement a fuzzy logic approach with different modulation index that can eliminate the selective harmonic [23]. A low THD is obtained for multi-level inverter when compared to the two-level inverter [24-26].

This paper covers the harmonic distortion of using multilevel inverter for a BLDC motor supplied by a PV array system. The main disadvantages of the MLI is the constraint of designing the control strategy for the PWM switching circuit. It is a challenge to adopt a solar PV with a multilevel inverter utilizing two topologies, diode clamped multilevel inverter, flying capacitor multilevel inverter that requires a huge number of switches. The control technique works based on space vector modulation switching technique. During the changing of the PV output voltage a high distortion might occur caused by the variation of the environment conditions and for that reason a MPPT introduced to avoid this problem.

2. MATHEMATICAL SYSTEM MODEL

The complete proposed system block diagram is shown in Figure 1. It includes PV array, boost dc-to-dc converter, 3-phase three level inverter, incremental conductance maximum power point tracking (INC-MPPT), SVPWM, and BLDC motor [27].

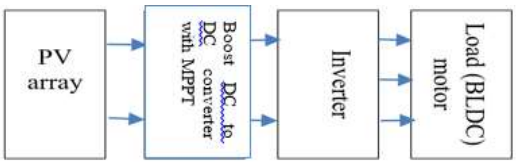

Figure 1. Block diagram for solar PV fed BLDC motor drive

2.1. PV Panel and INC- MPPT

The INC algorithm can be summarized as in flow chart as shown in Figure 2 and the simulation model of the implementation of INC with a solar PV boost dc to dc converter is shown in Figure 3. Since The INC algorithm employs the slope of the power-voltage curve of a PV array is equal to zero at the MPP [20] and [28]. The PV characteristics and the simulation results for PV model due to different of irradiance on the I-V and P-V characteristic at constant temperature (25 C°) as well as the effect of variation of temperature on the I-V and P-V characteristic at constant irradiance (1000W/m^2) are given in appendix A.

2.1.1. BLDC motor

For a BLDC motor, the direct and quadrature axis inductances are not equal, and the voltage equations are given as the following: There are three stator windings in the stator and a rotor consists of a permanent magnet of the BLDC. Due to the high resistivity rotor, the induced currents are neglected. The voltage equations for a 3-phase BLDC motor in matrix form are [27]:

$$\begin{bmatrix} V_a \\ V_b \\ V_c \end{bmatrix} = \begin{bmatrix} Rs & 0 & 0 \\ 0 & Rs & 0 \\ 0 & 0 & Rs \end{bmatrix} \begin{bmatrix} i_a \\ i_b \\ i_c \end{bmatrix} + \begin{bmatrix} L_{aa} & L_{ab} & L_{ac} \\ L_{ba} & L_{bb} & L_{bc} \\ L_{aa} & L_{cb} & L_{cc} \end{bmatrix} \frac{d}{dt} \begin{bmatrix} i_a \\ i_b \\ i_c \end{bmatrix} + \begin{bmatrix} e_a \\ e_b \\ e_c \end{bmatrix} \quad (1)$$

where v_a , v_b and v_c are the phase voltages ; i_a, i_b and i_c are the stator currents; e_a, e_b and e_c are the BEMFs; Rs is the stator winding resistance; L_{aa}, L_{bb} and L_{cc} are the self-inductances of the stator windings; L_{ab}, L_{ba}, L_{ac}, L_{ca}, L_{bc} and L_{cb} are the mutual inductances between the windings and No damper windings. By assuming

equal resistances and inductances for the phases, $L_{aa}= L_{bb} = L_{cc}= L$, $L_{ab} = L_{ba}= L_{ac}= L_{ca}= L_{bc} = L_{cb} =$, the following equations obtained:

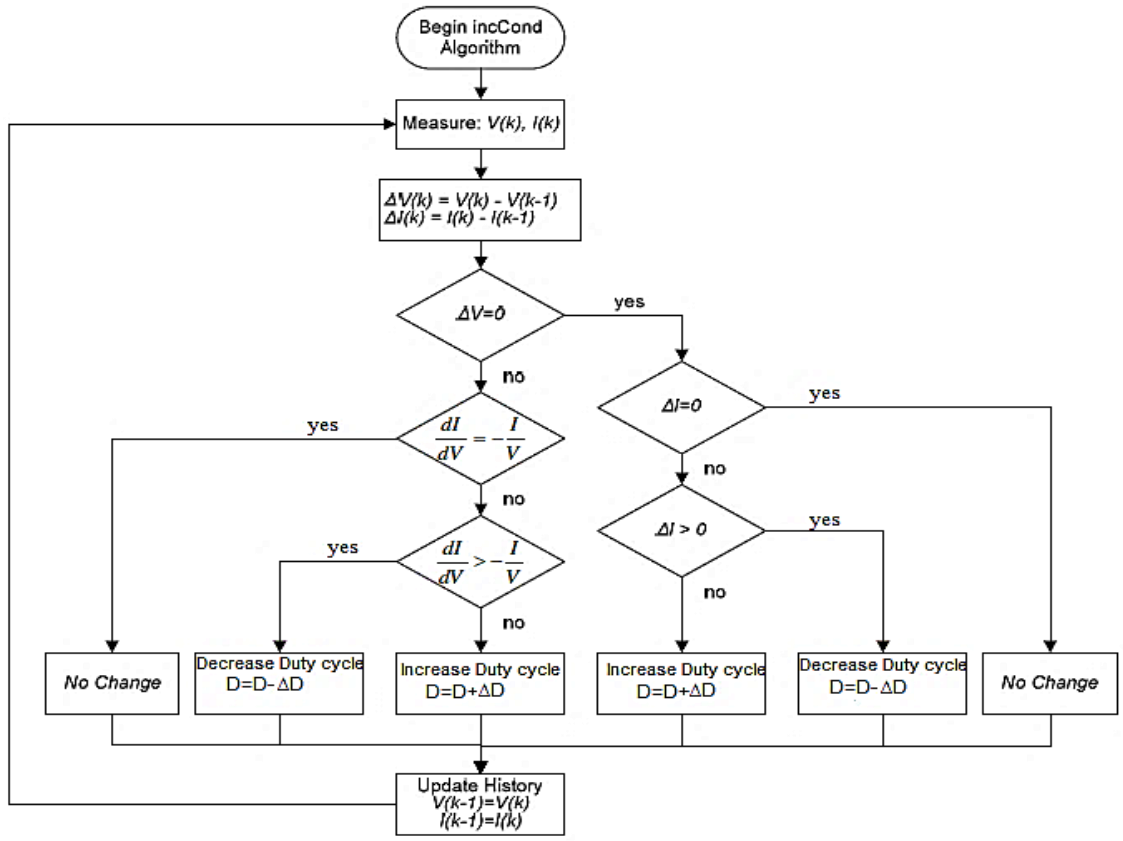

Figure 2. INC flow chart

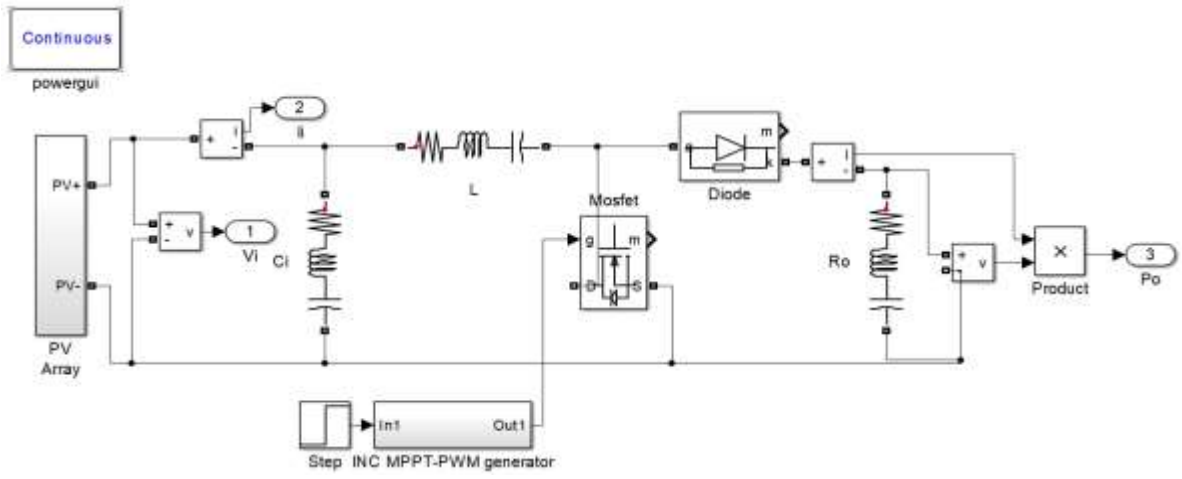

Figure 3. PV panel with boost converter model

$$\begin{bmatrix} V_a \\ V_b \\ V_c \end{bmatrix} = \begin{bmatrix} Rs & 0 & 0 \\ 0 & Rs & 0 \\ 0 & 0 & Rs \end{bmatrix} \begin{bmatrix} i_a \\ i_b \\ i_c \end{bmatrix} + \begin{bmatrix} L & M & M \\ M & L & L \\ M & M & L \end{bmatrix} \frac{d}{dt} \begin{bmatrix} i_a \\ i_b \\ i_c \end{bmatrix} + \begin{bmatrix} e_a \\ e_b \\ e_c \end{bmatrix} \quad (2)$$

The 3 stator phase currents are controlled to be balanced,

$ia + ib + ic = 0$ and $ib + ic = -ia$

$$\begin{bmatrix} V_a \\ V_b \\ V_c \end{bmatrix} = \begin{bmatrix} Rs & 0 & 0 \\ 0 & Rs & 0 \\ 0 & 0 & Rs \end{bmatrix} \begin{bmatrix} i_a \\ i_b \\ i_c \end{bmatrix} + \begin{bmatrix} L-M & 0 & 0 \\ 0 & L-M & 0 \\ 0 & 0 & L-M \end{bmatrix} \frac{d}{dt} \begin{bmatrix} i_a \\ i_b \\ i_c \end{bmatrix} + \begin{bmatrix} e_a \\ e_b \\ e_c \end{bmatrix} \quad (3)$$

The equations for the BEMFs for BLDC motor are given by:

$$\begin{bmatrix} e_a \\ e_b \\ e_c \end{bmatrix} = \omega_m \lambda_m \begin{bmatrix} f_a(\theta_r) \\ f_b(\theta_r) \\ f_c(\theta_r) \end{bmatrix} \quad (4)$$

Where ω_m the mechanical rotor speed in rad/sec,
λ_m is the magnetic flux linkage,
θ_r is the rotor position in radian and the functions $f_a(\theta_r), f_b(\theta_r) and\ f_a(\theta_r)$ with a trapezoidal shape having an amplitude of ±1.

The electromagnetic torque is given as:

$$T_e = \frac{e_a i_a + e_b i_b + e_c i_c}{\omega_m} \quad (5)$$

$$J \frac{d\omega_m}{dt} + B\omega_m = T_e - T_L \quad (6)$$

Where moment of inertia is *J*, friction coefficient is *B*, and load torque is T_L

The simulation schematic diagram is shown in Figure 4.

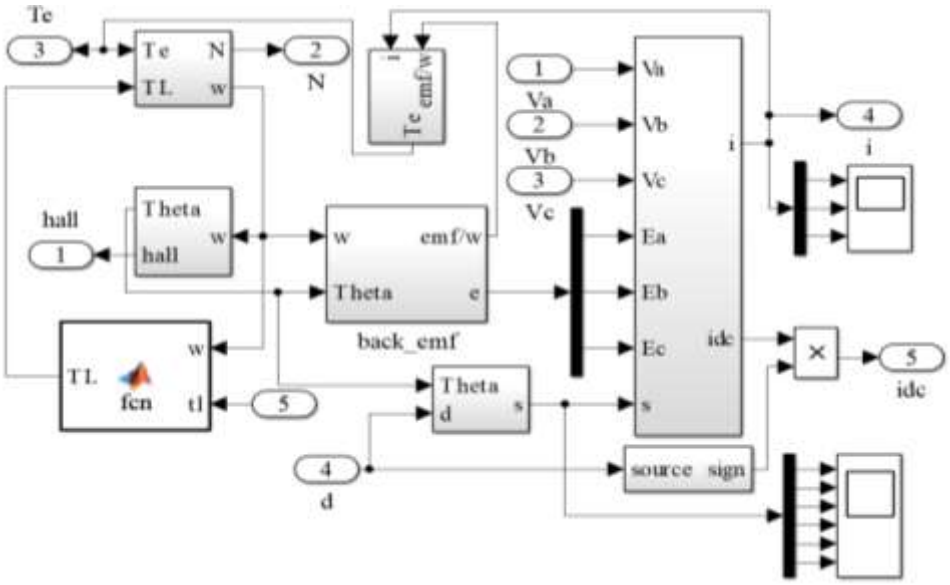

Figure 4. BLDC matlab/Simulink model

2.1.2. Three level inverter with SVPWM

Two inverter topologies have been considered in this paper; Figure 5 shows the schematic block diagram of the 3-phase three level diode clamped inverter topology [18]. Figure 6 shows the schematic block diagram of the 3-phase three level diode clamped inverter topology [29-31].

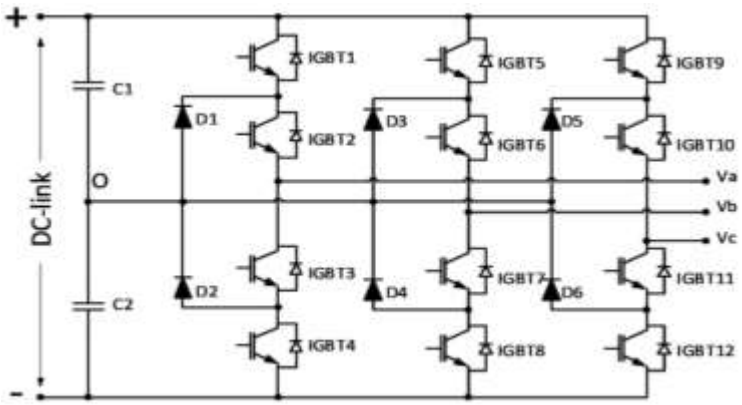

Figure 5. 3-phase three level diode-clamped inverter

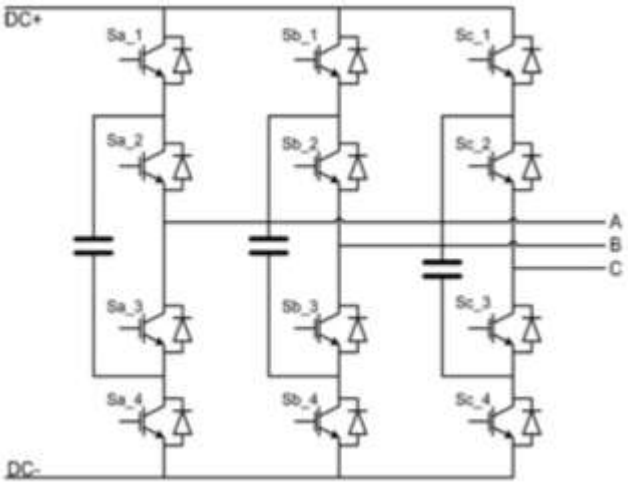

Figure 6. 3-phase three-level flying capacitor inverter

SVPWM technique is used extensively for its low switching loss, high flexibility and low computational complexity [17]. PWM technique finds the average variation of voltage space vector. The general structure is shown in the Figure 7. It can be shown that each inverter leg contains two switches, using the combination of these switches eight switching states will be generated that will produce a PWM waveform such that the average variation in the phase will be sinusoidal. In these switching states there are six active states and two zero states, and they can be represented as a hexagonal shape in a two dimensional plane. The hexagon is divided into six sectors the radius is equal to the voltage space vector of the three-phase inverter.

In Figure 7 the 3-phase output voltages are represented in one reference vector that is V_{ref} and this vector is rotating in an angular velocity $\omega = 2\pi f$. The main objective of the space vector modulation is to estimate the reference vector, and this can be done using the switching combination, the approximation is done by switching between any two adjacent active vectors and the zero or null vector. Based on that, the following equations are represented as:

$$T_1 V_1 + T_2 V_2 + T_0 V_{0,7} = T_S \, V_{ref} \quad (7)$$

$$T_1 + T_2 + T_0 = T_s \quad (8)$$

In which T_1, T_2 and T_0 are the duty-times for the active voltage vector V_1, V_2 and the zero-voltage vector $V_{0,7}$ in the one PWM period (T_s) is the switching time. In the space vector PWM a rotating voltage vector is used as a reference and this vector is sampled once in every sub cycle T_s. Based on the equations above there are two operating conditions for the inverter that is if $T_1 + T_2 < T_s, T_0 > 0$ then the inverter is

said to be in the linear modulation mode and this mode contains sufficient modulation margin to pursue the reference vector. When $T_1 + T_2 > T_s, T_0 < 0$ this is known as the over modulation mode.

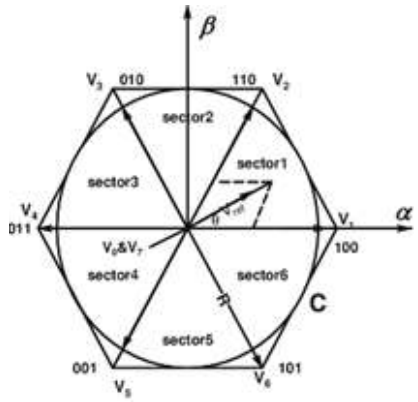

Figure 7. Eight switching states of the inverter

2.1.3. Simulation results and discussion

Matlab / Simulink simulation model is shown in Figure 8. The implementation is carried out on the motor that has parameters are given as the following: $R_s = 9.62 * 10^{-3}\Omega$, direct axis inductance $L_d = 28.7 * 10^{-6}H$, quadrature axis inductance $L_q = 47.2 * 10^{-6}H$, number of pole pair $P_b = 6$, moment of inertia J=20.17 kg.m^2, permanent magnet flux-linkage $\psi_m = 9.71 * 10^{-3}Wb$ and viscous friction coefficient B=0 N.m.s . The drive system uses a space vector PWM inverter with a switching frequency of 5kHz and dc-bus voltage of 200V.

The PV panel with its specifications that given as:

Peak power=300W; open circuit voltage=44.6V; MPP voltage= 36.34V; short circuit current= 8.7A; MPP current = 7.8A

The boost dc to dc converter parameters that given as:

Boost inductor= 2.2mH; DC bus capacitor=500 µF; switching frequency=20kHz.

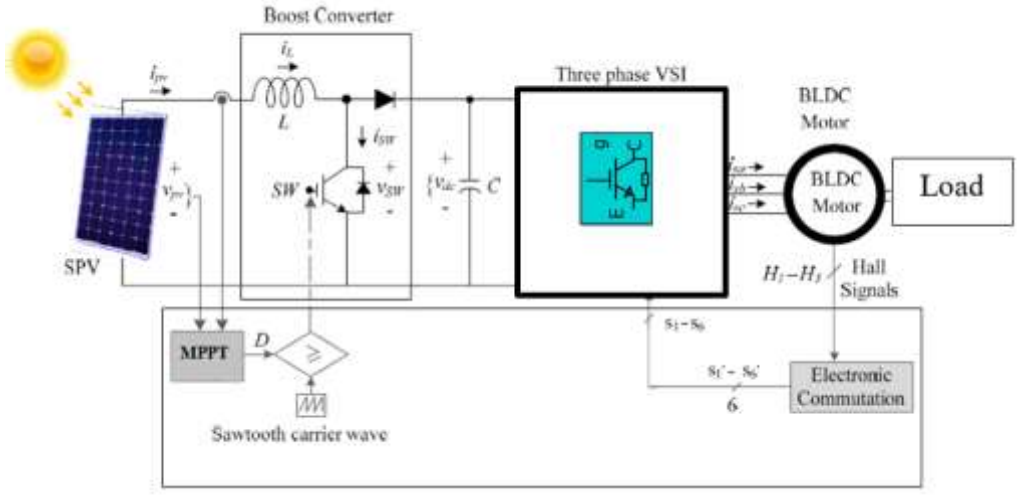

Figure 8. Block diagram control for solar PV fed BLDC motor drive

Case 1: 3-phase three level diode-clamped inverter

The simulation results inverter schematic diagram illustrated in Figure 1(a) that fed the BLDC motor and supplied from a PV with MPPT boost dc-to-dc converter. The line voltage waveforms are shown in

Figure 9. The 3-phase current signal and the harmonic spectra of the current signal at modulation index (MI) of 1.4 are shown in Figure 10(a) and (b). It can be achieved that the THD for the current signal is 5.27%.

From Figure 9(b), it can be seen that there is a clear trend of decreasing THD to 5.27% when a multilevel inverter is implemented. This result is significant at the irradiance of 1000W/m2 at 25C°.

Case 2 : 3-phase three-level flying capacitor inverter

The simulation results inverter schematic diagram illustrated in Figure 1(b) that fed the BLDC motor and supplied from a PV with maximum power point tracking boost dc-to-dc converter. The line voltage waveforms are shown in Figure 11. The 3-phase current signal and the harmonic spectra of the current signal at modulation index of 1.4 are shown in Figure 12(a) and (b). It can be achieved that the THD for the current signal is 13.92%. It is difficult to explain this result, but it might be related to unbalanced voltage.

For the above results, when the three level inverter is operating under steady state conditions with SVPWM within a switching interval for each inverter. Together these results provide and indicate an important insights into switching losses that associated with the flying capacitor inverter has a higher compared to diode clamped inverter. In addition, in order to overcome the MI limitation in SVPWM, the isolated dc voltage has to be modified to improve the voltage profile.

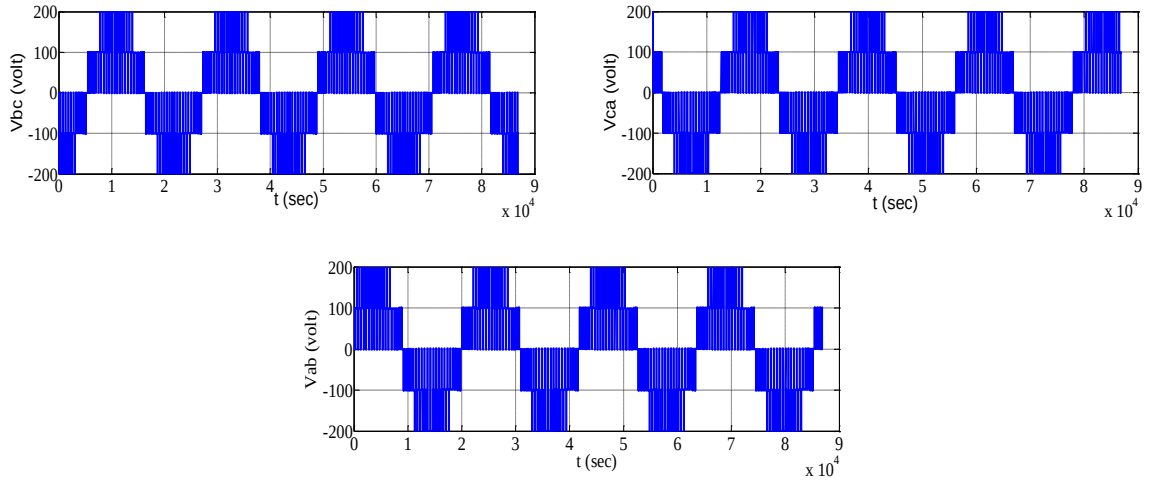

Figure 9. Simulation results of voltage

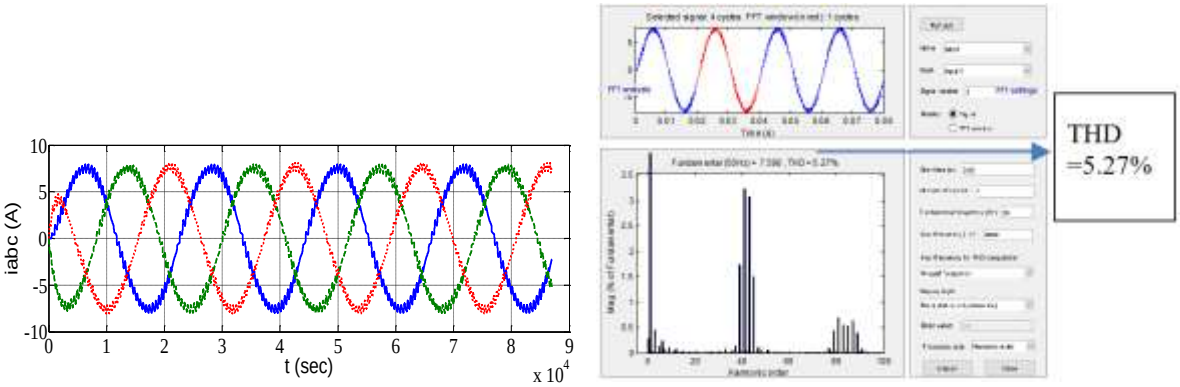

Figure 10. (a) Simulation results of 3-phase current (b) Harmonic spectra for current signal

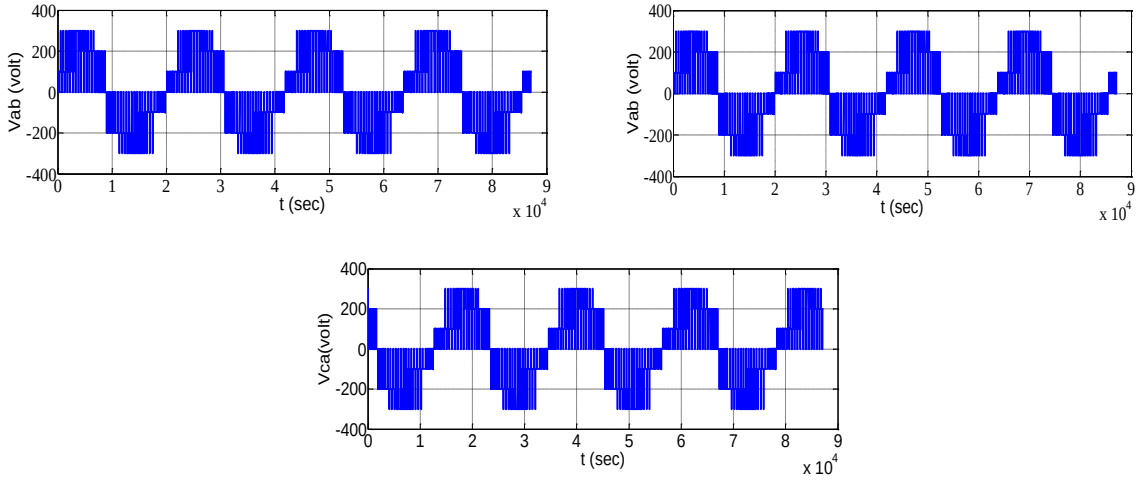

Figure 11. Simulation results of voltage

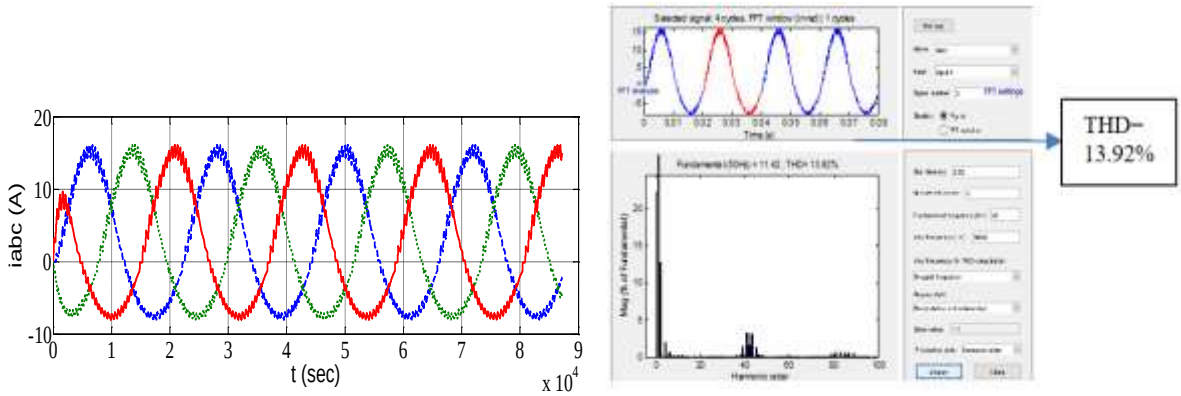

(a) (b)

Figure 12. (a) Simulation results of 3-phase current (b) Harmonic spectra for current signal

3. CONCLUSION

This paper discusses the 3-phase three level inverter topologies that implemented with a solar PV fed a BLDC motor drive. In order to prove their effectiveness respecting the primarly objective to current THD, and they can be used in industrial applications. The results have shown an improved utilization of the dc-bus voltage, still the overshoot is a little bit high in two types of inverter that are proposed. It has been seen that the multilevel clamped diode inverter type can work with a good dynamic comparing to flying capacitor inverter type. The simulation results suggest that a multilevel inverter can be develop THD. It is also showed that a good quality of voltage signal can be obtained for 3-phase three level diode-clamped inverter about 5.2% compared with that Of THD 13.92% for flying capacitor inverter. It can be concluded that clamped diode inverter topology is efficient as it assures satisfy harmonic distortion. A Matlab/Simulink was carried out to model the system.

REFERENCES

[1] Duane Hanselman, “Brushless permanent magnet motor design”, 2nd edition, Magna Physics publishing, 2006.
[2] Shivam Maurya Deptt.,Dheeraj Mishra Deptt., Kavita Singh Deptt., A K Mishra Rajkiya, and Yudhisthir Pandey "An Efficient Technique to reduce Total Harmonics Distortion in Cascaded H- Bridge Multilevel Inverter", *IEEE International Conference on Electrical, Computer and Communication Technologies (ICECCT)*, 20-22 Feb. 2019.
[3] Auzani Jidin, Syamim Sanusi, Tole Sutikno, Nik Rumzi Nik Idris,"Improved Output Voltage Quality using Space Vector Modulation for Multilevel Inverters", *TELKOMNIKA (Telecommunication, Computing, Electronics and Control)*, vol 14, no 2, Dec 2017.
[4] Arikesh A., A. K. Parvathy," Modular multilevel inverter for renewable energy applications", *International Journal of Electrical and Computer Engineering (IJECE)*, vol 10, no 1, 2020 (PART I).

[5] Kamel Saleh,"Photovoltaic Integrated Unified Power Quality conditioner with a 27-level Inverter", *TELKOMNIKA (Telecommunication, Computing, Electronics and Control, Institute of Advanced Engineering and Science)*, vol. 17, 2019.
[6] Karthikeyan, D.Palanisamy, R.,Vijayakumar, K.;Velu, A.;Selvabharathi, D.,"Parallel Connected VSI Inverter using Multi-carrier based Sinusoidal PWM Technique", *TELKOMNIKA (Telecommunication, Computing, Electronics and Control, Institute of Advanced Engineering and Science)*, vol 15, no 4, 2017.
[7] Hani Vahedi, Philippe-Alexandre Labbe, Kamal Al-Haddad. "Balancing Three-Level NPC Inverter DC Bus Using Closed-Loop SVM: Real Time Implementation and Investigation", *IET Power Electron*. pp. 1–9 & the Institution of Engineering and Technology, 2016.
[8] Amol K. Koshti, M. N. Rao," A brief review on multilevel inverter topologies", *International Conference on Data Management, Analytics and Innovation (ICDMAI)*, 24-26 Feb. 2017.
[9] AMA Hussain, HMD Habbi, "Design and Performance Analysis of a 3-Phase Induction Motor for Solar Photovoltaic Fed Pumping System", *Journal of Engineering and Applied Sciences*, vol. 15, no. 3, pp. 773-782, 2020.
[10] Deekshitha S Nayak, R Shivarudraswamy," Solar fed BLDC motor drive for mixer grinder using a boost converter," *International Journal of Power Electronics and Drive Systems (IJPEDS)*, vol 11, no 1, 2020.
[11] Kishor Thakre, Kanungo Barada Mohanty, Haris Ahmed, Ashwini Ku Nayak," Modified Cascaded Multilevel Inverter with Reduced Component Count," 2017 14th *IEEE India Council International Conference (INDICON)*, 2017.
[12] Muralidhar Nayak Bhukya, Venkata Reddy Kota, Shobha Rani Depuru," A Simple, Efficient, and Novel Standalone Photovoltaic Inverter Configuration with Reduced Harmonic Distortion", *IEEE Access*, vol. 7, pp. 43831-43845, 2019.
[13] Yoganandini A. P., Anitha G. S,"A modified particle swarm optimization algorithm to enhance MPPT in the PV array," *International Journal of Electrical and Computer Engineering (IJECE)*, vol 10, no 5, 2020 (Part II).
[14] Weidong Jiang, Xinmei Huang, Jinping Wang, Jianing Wang, Jinsong Li," A Carrier-Based PWM Strategy Providing Neutral-Point Voltage Oscillation Elimination for Multi-Phase Neutral Point Clamped 3-Level Inverter", *IEEE Access*, vol 7, pp. 124066–124076, 2019.
[15] Anyuan Ye, Le Chen, Lixuan Kang, Song Li, Junfei Zhang, Han Wu," Hybrid Multi-Carrier PWM Technique Based on Carrier Reconstruction for Cascaded H-bridge Inverter", *IEEE Access*, vol 7, pp. 53152-53162, 2019.
[16] Hadik Azeem, Suresh Yellasiri, Venkatramanaiah Jammala, Banavath Shiva Naik, Anup Ku," A Fuzzy Logic Based Switching Methodology for a Cascaded H-Bridge Multi-Level Inverter", *IEEE Transactions on Power Electronics*, vol. 34, no. 10, pp. 9360-9364, 2019.
[17] Jiangbiao He, Cong Li, Anoop Jassal, Naveenan Thiagarajan, Yichao Zhang, Satish Prabhakara, Carlos Feli, James E. Graham, Xiaosong Kang "Multi-Domain Design Optimization of dv/dt Filter for SiC-Based Three-Phase Inverters in High-Frequency Motor-Drive Applications", *IEEE Transactions On Industry Applications*, vol. 55, no. 5, 2019.
[18] Ning Li, Wanting Li, Hui Zhang, Ping Yang," Efficiency-optimised modulation technique of three-level NPC inverter", *The Journal of Engineering*, vol. 2019, no. 3, pp. 938-942, 2019.
[19] R. Palanisamy, K. Selvakumar, K. Vijayakumar, D. Karthikeyan, S. Vidyasagar, V. Kalyanasundaram, "Transformer based NPC multilevel inverter using reduced number of components", *International Journal of Electrical and Computer Engineering (IJECE)*, vol. 9, no. 6, 2019 (Part II).
[20] Mostafa Mosa, Mohammad B. Shadmand, Robert S. Balog, Haitham Abu Rub," Efficient maximum power point tracking using model predictive control for photovoltaic systems under dynamic weather condition", *IET Renewable Power Generation*, vol. 11, no. 11, pp. 1401-1409, 2017.
[21] Jon Azurza Anderson, Eli J. Hanak, Lukas Schrittwieser, Mattia Guacci, Johann W. Kolar, Gerald Deboy," All-silicon 99.35% efficient three-phase seven-level hybrid neutral point clamped/flying capacitor inverter", *CPSS Transactions on Power Electronics and Applications*, vol. 4, no. 1, pp. 50-61, 2019.
[22] Kokila Arunachalam, Senthil Kumar Vairakannu, Gobi Nallathambi," Comparison and optimisation of three-level neutral point clamped dual output inverter", *IET Circuits, Devices & Systems*, vol. 14, no. 1, pp. 48–59, 2020.
[23] Alian Chen, Zicheng Zhang, Xiangyang Xing, Ke Li, Chunshui Du, Chenghui Zhang," Modeling and Suppression of Circulating Currents for Multi-Paralleled Three-Level T-Type Inverters", *IEEE Transactions on Industry Applications*, vol. 55, no. 4, pp. 3978-3988, 2019.
[24] Reza Khamooshi, Alireza Namadmalan," Converter utilisation ratio assessment for total harmonic distortion optimisation in cascaded H-bridge multi-level inverters", *IET Power Electronics*, vol. 9, no. 10, pp. 2103-2110, 2016.
[25] Suresh N., R. Samuel Rajesh Babu," Reduction of Total Harmonic Distortion in Cascaded H-Bridge Inverter by Pattern Search Technique", *International Journal of Electrical and Computer Engineering (IJECE)*, vol. 7, no. 6, 2017.
[26] Arikesh A., A. K. Parvathy,"Modular multilevel inverter for renewable energy applications", *International Journal of Electrical and Computer Engineering (IJECE)*, vol. 10, no. 1, 2020 (PART I).
[27] G. G. Raja Sekhar, Basavaraja Banakara," An Internal Current Controlled BLDC Motor Drive Supplied with PV Fed High Voltage Gain DC-DC Converter", *International Journal of Electrical and Computer Engineering (IJECE)*, vol. 8, no. 2, 2018.
[28] Gaddala Jayaraju, Gudapati Sambasiva Rao, "Intelligent controller based power quality improvement of microgrid integration of photovoltaic power system using new cascade multilevel inverter", *International Journal of Electrical and Computer Engineering (IJECE)*, vol. 9, no. 3, 2019.
[29] Ezzidin Hassan Aboadla, Sheroz Khan, Mohamed H. Habaebi, Teddy Surya Gunawan, Belal A. Hamida, Mashkuri Bin Yaacob, Ali Aboadla," A novel optimization harmonic elimination technique for cascaded multilevel inverter", *Bulletin of Electrical Engineering and Informatics (BEEI)*, vol. 8, no. 2, 2019.
[30] Kamel Saleh, Nael Hantouli,"A photovoltaic integrated unified power quality conditioner with a 27-level inverter", *TELKOMNIKA (Telecommunication, Computing, Electronics and Control)*, vol. 17, no. 6, 2019.
[31] Liangzong He, Chen Cheng," A Flying-Capacitor-Clamped Five-Level Inverter Based on Bridge Modular Switched-Capacitor Topology", *IEEE Transactions on Industrial Electronics*, vol. 63, no. 12, pp. 7814-7822, 2016.

BIOGRAPHY OF AUTHOR

Afaneen Alkhazragy received the B.Sc. degree in electrical engineering from University of Baghdad in 1990. She received her M.Sc. and PhD degrees in electrical engineering, Power engineering from University of Technology, Baghdad, Iraq, in 1998 and 2005 respectively. From 1993 till now, she was a faculty member with the Electrical engineering department, University of Technology. Since 2005, she has been as assistance professor. Her research interest includes power engineering, power system analysis, power system operation and control, and power quality.

Appendix A PV characteristics simulation results.
Figure A-1 shows the variation of irradiance on I-V and P-V characteristic at constant temperature. Figure A2 shows Different of temperature on the I-V and P-V characteristic at constant irradiance.

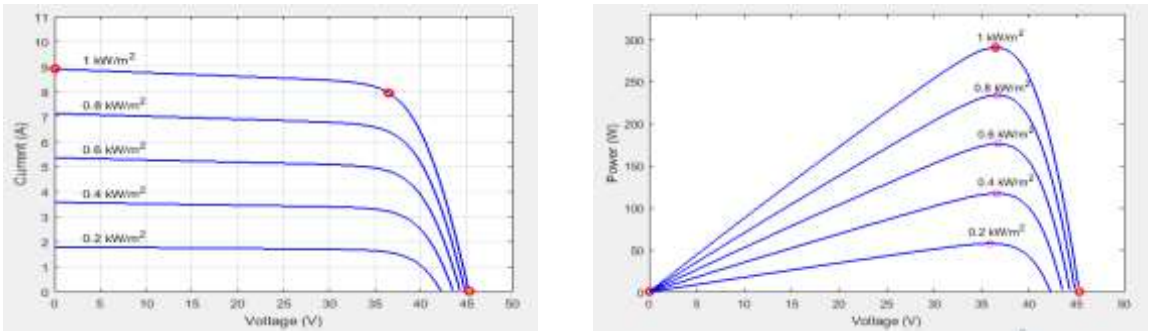

Figure A1. Different of irradiance on the I-V and P-V characteristic at constant temperature (25^0)

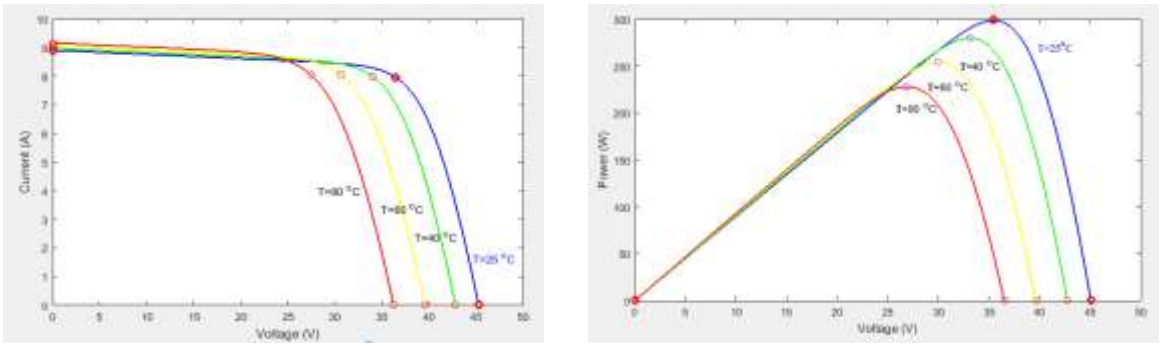

Figure A2. Different of temperature on the I-V and P-V characteristic at constant irradiance ($1000W/m^2$)